MULTISCALE CHARACTERIZATION OF RESERVOIR ROCK MICROSTRUCTURE: COMBINING SMALL-ANGLE NEUTRON SCATTERING AND IMAGE ANALYSIS

A.P. Radlinski [(1)], M.A. Ioannidis [(2)], A. L. Hinde [(1)] , M. Hainbuchner [(3)], M. Baron [(4)], H. Rauch [(3)], and S. R. Kline [(5)]

[(1)] Geoscience Australia, Canberra City, Australian Capital Territory 2601, Australia
[(2)] University of Waterloo, Waterloo, Ontario N2L 3G1, Canada
[(3)] Atominstitut der Österreichischen Universitäten, A-1020, Wien, Austria
[(4)] Institute Max von Laue - Paul Langevin, F-38042 Grenoble Cedex , France
[(5)] NIST Center for Neutron Research, Gaithersburg, MD 20899, USA

ABSTRACT

The correlation function and the absolute neutron scattering cross section are obtained for a sample of reservoir sandstone in the linear scale range 10 Å to 1 mm by combining small-angle neutron scattering data (SANS/USANS) with statistical analysis of backscatter scanning electron micrographs (BSEM) of the pore space. The pore-rock fabric interface is a surface fractal (D = 2.47) over 4 orders of magnitude of the length scale and 15 orders of magnitude in scattering intensity, with an upper limit cut-off of about 40 μm. The specific surface area, pore size distribution and total porosity, calculated along the lines of a polydisperse spherical pore (PDSP) model, are consistent with mercury porosimetry data. The PDSP analysis quantifies the fraction of pore volume in the fractal regime and illustrates the possibility of characterizing the microgeometry in terms of a continuous pore size distribution, covering length scales from few nanometers to hundreds of microns. Such information is useful in the interpretation of special core analysis data, as illustrated for the case of the NMR-T_2 distributions for the sample studied.

INTRODUCTION

Adequate understanding of pore geometry underlies all efforts to predict the capillary properties of reservoir rock. The significance of properly accounting for the smallest as well as the largest pore length scales is nowhere more evident than in attempts to predict the amount of capillary-bound water (Song *et al*., 2000) or to explain the rate and extent of spontaneous imbibition (Constantinides and Payatakes, 2000). A quantitative geometric description is, however, very difficult because the pore space of sedimentary rock comprises a very broad distribution of length scales, ranging from nanometers to hundreds of micrometers.

The simplified picture of porous sedimentary rock as a collection of compacted grains is often successfully employed to explain the absolute permeability of sandstones (Bryant *et al*., 1993). However, such a picture does not account for the enormous variability of pore length scales present and for this reason generally fails to explain capillary properties. In fact, these materials are some of the most extensive surface fractal systems found in nature (Radlinski *et al*., 1999). Still, only a fraction of the total pore volume in sedimentary rock is accounted for by a surface fractal, hence knowledge of the surface fractal dimension is insufficient to describe the geometry at all relevant scales. An experimentally validated picture of sedimentary rock, which honors length scales of the order of the grain size, as well as length scales associated with microporosity is still lacking.

No single experimental technique can provide a quantitative description of rock micro-architecture over length scales spanning four to five orders of magnitude, as required. Direct imaging methods, such as backscatter scanning electron microscopy (BSEM) (Ioannidis *et al*., 1996) and X-ray microtomography (Spanne *et al*., 1994) become unwieldy for providing statistically significant microstructure data at length scales smaller than about 1 micrometer. These methods are not well suited for the study of the surface fractal characteristics of sedimentary rocks. Indirect imaging methods, like small-angle neutron scattering (SANS/USANS) or small-angle X-ray scattering (SAXS), yield the volume-averaged Fourier transform of the density correlation function on length scales ranging from one nanometer to about 10 micrometers (Radlinski *et al*., 1999). Greater length scales, accounting for much of the pore volume in sedimentary rock, cannot be probed by these techniques. Alternatively, the pore space may be invasively probed by liquids, using mercury intrusion porosimetry (MIP) – a method providing information about the distribution of pore volume by pore throat size in the range 20 nm to 100 μm - or by adsorption and capillary condensation experiments (Broseta *et al*., 2001). Nuclear magnetic resonance (NMR) relaxation (Kenyon, 1997) and diffusion (PFG-NMR) experiments may also be employed to probe the geometry of the pore space in a non-invasive manner.

The most general description of a porous medium is in terms of a statistical phase function $Z(\mathbf{x})$, taking the value of unity if $\mathbf{x}$ points to solid and zero otherwise. The first two moments of $Z(\mathbf{x})$ are the porosity, $\phi = \langle Z(\mathbf{x}) \rangle$ and the two-point correlation function, $S_2(\mathbf{r}) = \langle Z(\mathbf{x}) Z(\mathbf{x}+\mathbf{r}) \rangle$, where $\mathbf{r}$ is a lag vector and angular brackets denote statistical averages. For isotropic media the two-point correlation function depends only on the modulus of the lag vector, i.e. $S_2(\mathbf{r}) = S_2(r)$. For length scales greater than about 1 μm, the function $S_2(r)$ is readily determined by statistical analysis of binary micrographs of the pore space (Ioannidis *et al*., 1996). In small-angle scattering experiments, the scattering intensity is the Fourier transform of the density-density correlation function $\gamma(r)$:

$$I(Q) = \frac{d\sigma}{d\Omega}(Q) = 4\pi \int_0^\infty r^2 \gamma(r) \frac{\sin(Qr)}{Qr} dr \quad (1)$$

where $\gamma(r) = (\Delta\rho)^2 \phi(1-\phi) R_Z(r)$, $R_Z(r) \equiv (S_2(r) - \phi^2)/(\phi - \phi^2)$ is the void-void autocorrelation function and Q is the scattering angle. For neutron scattering in sedimentary rocks, regardless of their organic matter content, the scattering length density contrast, $(\Delta\rho)^2$, between various rock components is small compared to the contrast between any of these components and the void (Radlinski *et al*., 1999). Therefore, rocks scatter neutrons as a quasi-two-phase system. Consequently, the function I(Q) measured by SANS/USANS and the function $S_2(r)$ calculated from BSEM images, are a Fourier transform pair. It is on this basis that small-angle scattering and imaging information may be combined to obtain the scattering cross section I(Q) in the range $10^{-7} < Q < 10^{-1}$ Å^{-1}. Inverse Fourier transform then yields the autocorrelation $R_Z(r)$ in the size range 10 Å < r < 1 mm:

$$R_Z(r) = \frac{1}{2\pi^2 (\Delta\rho)^2 \phi(1-\phi)} \int_0^\infty Q^2 I(Q) \frac{\sin(Qr)}{Qr} dQ \quad (2)$$

Several alternatives exist for analyzing the I(Q) data. For a surface fractal object of dimension D, the scattering intensity follows the power-law $I(Q) \propto Q^{D-6}$. Alternatively, a theoretical model of the autocorrelation function for surface fractals with correlation length ξ (upper limit for the length of scale invariance) is (Mildner and Hall, 1986):

$$R_Z(r) = \exp\left(-\frac{r}{\xi}\right)\left[1 - C\left(\frac{r}{\xi}\right)^{3-D}\right] \quad (3)$$

where C is a constant. Fourier transform of Eq. (3) leads to the following analytical expression for the scattering intensity:

$$I(Q) \propto Q^{-1}\, \Gamma(5\text{-}D)\, \xi^{5-D}\, [1+(Q\,\xi)^2]^{(D-5)/2}\, \sin[(D\text{-}1)\arctan(Q\,\xi)] \quad (4)$$

A more versatile analysis is based on an approximation of the pore space as an arbitrary distribution of spheres of radius r (Radlinski *et al*., 2001). According to this model, hereafter referred to as the polydisperse spherical pore (PDSP) model, I(Q) is given by:

$$I(Q) = (\Delta\rho)^2 \frac{\phi}{\langle V_r \rangle} \int_{R_{min}}^{R_{max}} V_r^2 f(r) F_S(Qr) dr \quad (5)$$

In Eq. (5), R_{max} and R_{min} are the maximum and minimum pore radii, respectively, $V_r \equiv V(r) = (4/3)\pi r^3$ is the volume of a sphere of radius r, $\langle V_r \rangle = \int_{R_{min}}^{R_{max}} V_r f(r) dr$ is the

average pore volume, f(r) is the probability density of the pore size distribution, and $F_S(Qr)$ is the form factor for a sphere of radius r:

$$F_S(Qr) = \left[3\frac{\sin(Qr) - Qr\cos(Qr)}{(Qr)^3} \right]^2 \quad (6)$$

If the pore space is fractal, the pore size distribution follows the law $f(r) \propto r^{-(D+1)}$.

EXPERIMENTAL METHODS

A sandstone sample originating from the reservoir section of an oil well in central Australia was investigated (porosity ϕ = 0.181 and permeability k = 450 mD, by standard core analysis). XRD analysis indicated that the sample contained 98±0.39% quartz, 0.6±0.12% dickite, 1.50±0.37% mica (possibly muscovite) and 0.0±0.03% montmorillonite. SANS measurements were performed on instrument NG7 at NIST using a wavelength of 5 Å ($10^{-3} < Q < 10^{-1}$ Å^{-1}). This instrument is described in Glinka *et al*. (1986). USANS measurements were performed on instrument S18 (Austrian beam line, Grenoble Research Reactor, Grenoble, France) using a wavelength of 1.89 Å ($10^{-5} < Q < 10^{-3}$ Å^{-1}). This instrument is described in Hainbuchner *et al*. (2000). The neutron scattering experiments were performed on a 2-mm thick sample. Two sets of high-contrast BSE micrographs (100X magnification) were obtained from two perpendicular sections through the sample (65 images each). No significant difference in the statistical properties of the two sets was found and the measured autocorrelation functions were pooled into a single average. Additional images were obtained at a 500X magnification. Finally, the sample was studied by mercury intrusion porosimetry (MIP) and NMR relaxometry. The latter measurements were conducted on a fully water-saturated sample at 26.6 MHz using the Carr-Purcell-Meiboom-Gill pulse sequence with echo spacing of 0.5 ms on a modified Bruker SXP spectrometer.

RESULTS AND DISCUSSION

Typical BSEM images of the sample are shown in Figure 1. To within a constant equal to $(\Delta\rho)^2\phi(1-\phi)$, we computed I(Q) in the range $10^{-7} < Q < 10^{-4}$ Å^{-1} from $R_z(r)$ according to Eq. (1). The Q-range covered by the BSEM data overlaps the range covered by USANS and this permitted the determination of the constant $(\Delta\rho)^2\phi(1-\phi)$. When the BSEM and SANS/USANS data are combined, the absolute neutron scattering cross section is determined in the range $10^{-7} < Q < 10^{-4}$ Å^{-1}. The three methods span the linear size range 20 Å to 600 μm, which extends over the entire range of pore sizes in typical sandstones and is the widest continuous range ever studied for a sedimentary rock. The combined experimental data and the model fits are shown in Figure 2. For this sample, $\Delta\rho = 3.9\times10^{-10}$ cm^{-2} and we obtain ϕ = 0.184 from the invariant $\mathcal{I}$:

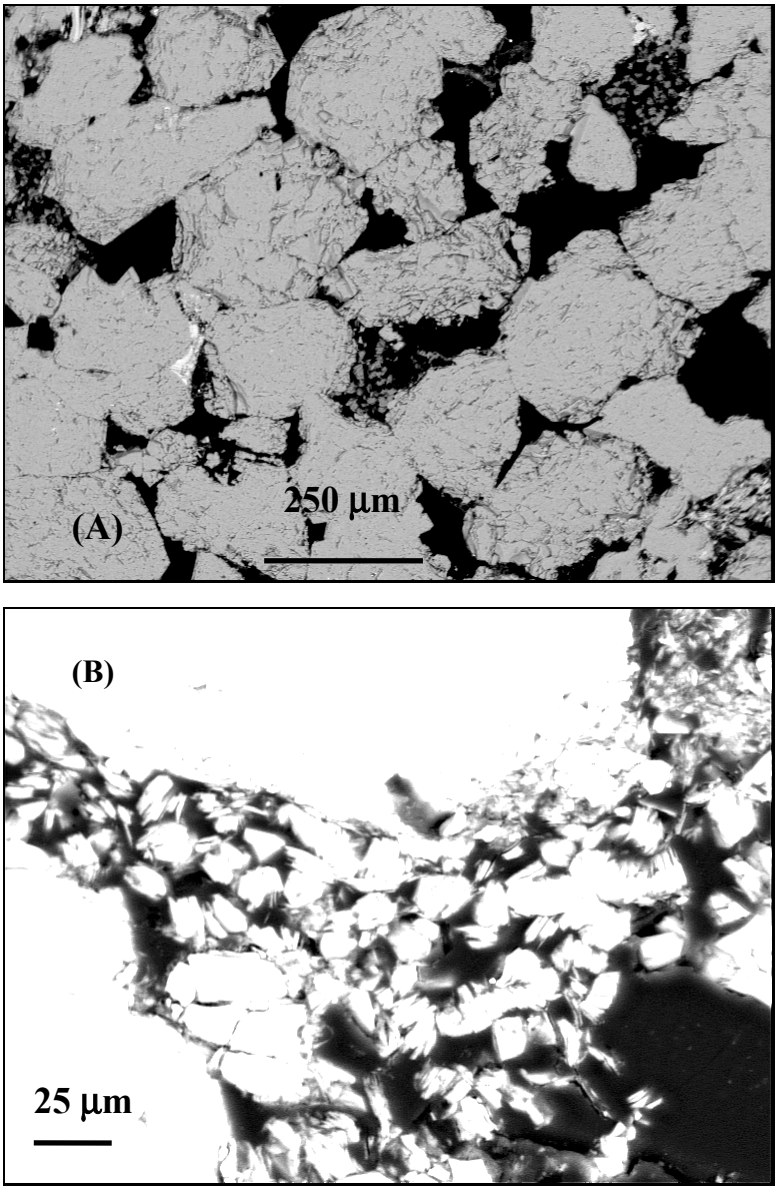

Fig. 1. (A) Typical BSE image used for statistical analysis (resolution of 1.55 μm/pixel). (B) Higher resolution image (0.31 μm/pixel) illustrating microporosity.

$$\mathcal{I} = \int_0^\infty Q^2 I(Q) dQ = 2\pi^2 (\Delta\rho)^2 \phi(1-\phi) \tag{7}$$

and $\phi = 0.181$ from the PDSP model fit:

$$\lim_{Q\to 0} I(Q) = (\Delta\rho)^2 \phi \frac{\langle V_r^2 \rangle}{\langle V_r \rangle} \tag{8}$$

Both of these values are in excellent agreement with the porosity determined by standard core analysis (0.181) and also with the porosity estimated by MIP at the maximum intrusion pressure of 60,000 psia ($\phi_{MIP} = 0.176$). These results confirm that the entire pore volume of the sample was probed by the combination of BSEM, USANS and SANS methods.

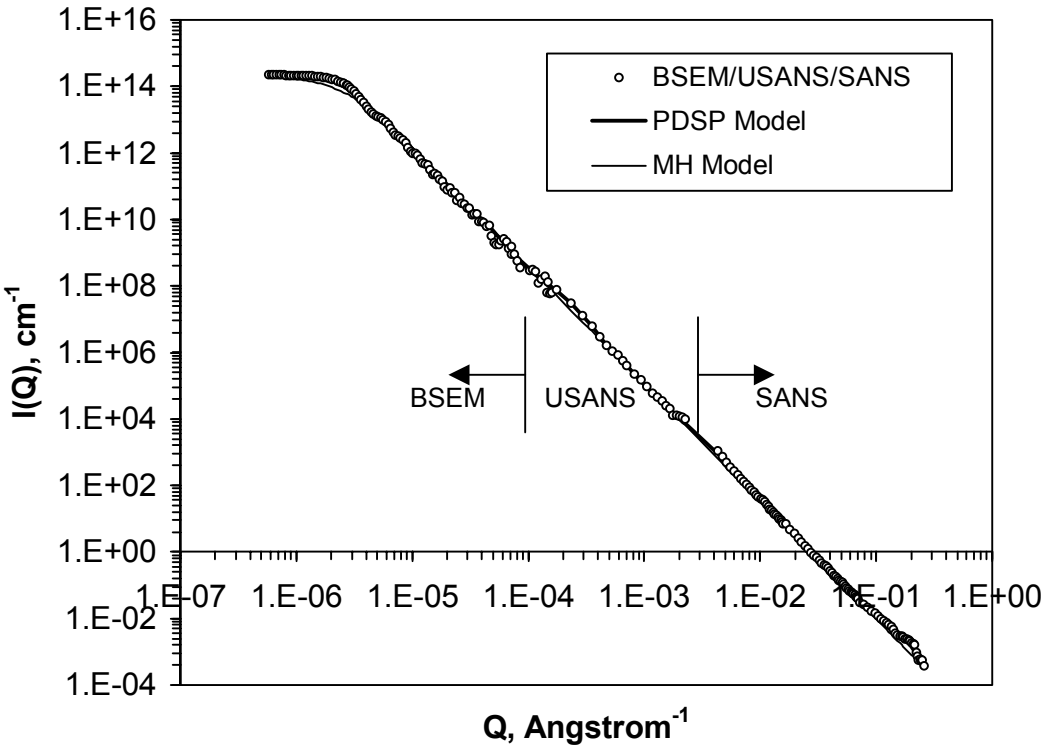

Figure 2. Experimentally determined absolute neutron scattering cross section I(Q) and fit by the polydispersed spherical pore (PDSP) model, Eq. (5), and by the Mildner-Hall (MH) model, Eq (4).

A fit of the scattering curve according to $I(Q) \propto Q^{D-6}$ indicates a very extensive surface fractal system (D = 2.5) with an upper cut-off that is roughly equal to 50 μm ($Q \approx 2\times10^{-6}$ Å^{-1}). A similar conclusion is reached when the I(Q) data are analyzed according to the MH model, Eq. (4): D = 2.47 and ξ = 35 μm. The MH model is based on the assumption that for small Q (large r) the correlations decay exponentially. In fact, the decay of correlations for large r in reservoir rock generally follows a stretched-exponential law (Ioannidis *et al.*, 1996). The function $R_z(r)$, recovered in the size range 10 Å < r < 1 mm by inverse Fourier transform of the combined I(q) data, is shown in Figure 3. Two salient features emerge. First, the MH model begins to breakdown for r-values greater than a few μm. Second, the function $R_z(r)$ determined from the BSE micrographs coincides with the complete $R_z(r)$ only beyond the fractal regime (r > 40 μm).

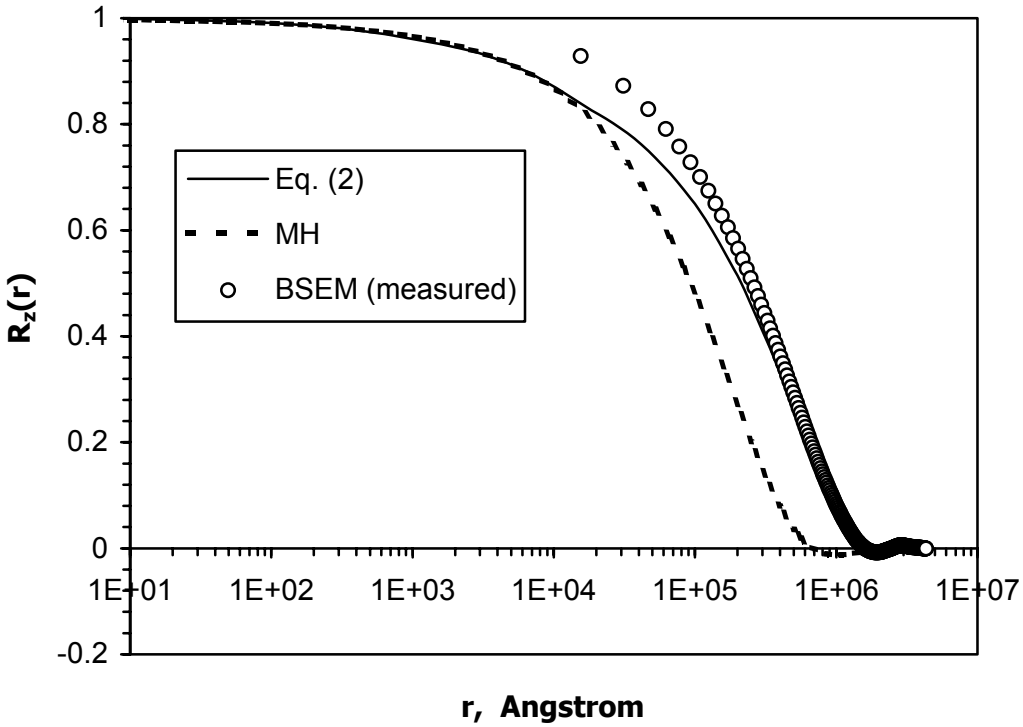

Figure 3. Void-void autocorrelation function $R_z(r)$. The comparison illustrates contributions to correlation by non-fractal objects of size greater than about 50 μm.

The pore size and surface area distributions according to the PDSP model are shown in Figure 4. According to this model, D = 2.49±0.03 and ξ = 60 μm, in agreement with the other estimates. Importantly, the PDSP analysis shows that the fraction of the pore volume associated with the surface fractal regime is approximately 62%. The specific surface area of the sample according to the PDSP model is S/V_p = 1.64 μm^{-1} – of the same order of magnitude as the value determined by MIP (S/V_p = 0.47 μm^{-1}). The lower value obtained by MIP is understood if one considers that this method does not account for contributions to the surface area by pores smaller than about 20 nm.

A synthetic mercury-air drainage capillary pressure curve can be simply constructed from the cumulative distribution of pore volume by pore size that is determined from the combined SANS/USANS/BSEM data by virtue of the PDSP model fit. To this end, the Young-Laplace equation, $P_c = 2\sigma\cos\theta / r$, provides the relationship between pore radius and capillary pressure, where σ is the surface tension of mercury (485 mN/m) and θ is the receding contact angle (40^o). A comparison of the synthetic curve with the experimental MIP data for this sandstone is shown in Figure 5. The two curves have similar shape and

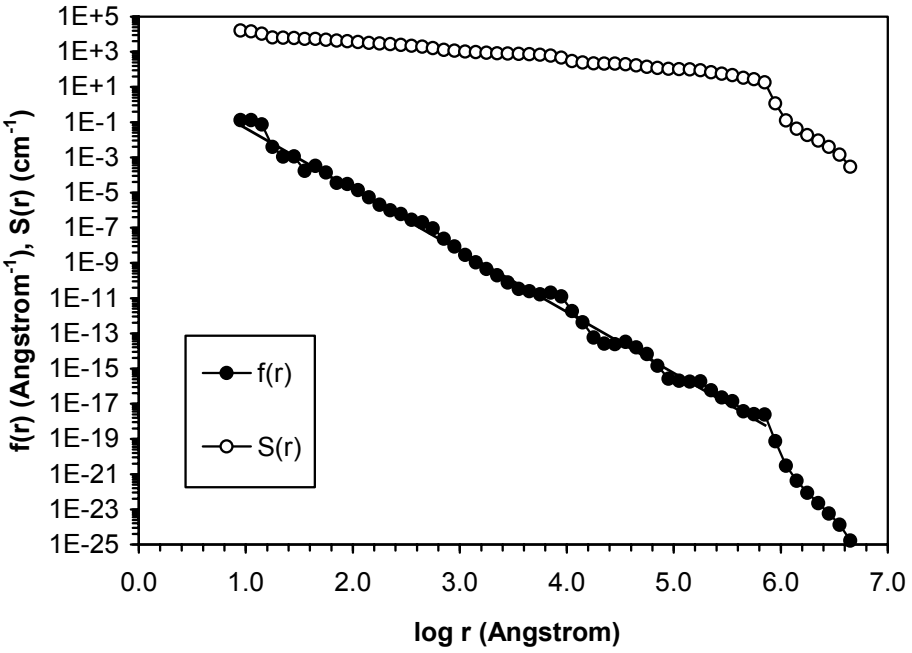

Figure 4. Distributions of pore size and specific surface area from PDSP model fit of scattering data. Straight line has slope -(D+1) = -3.49.

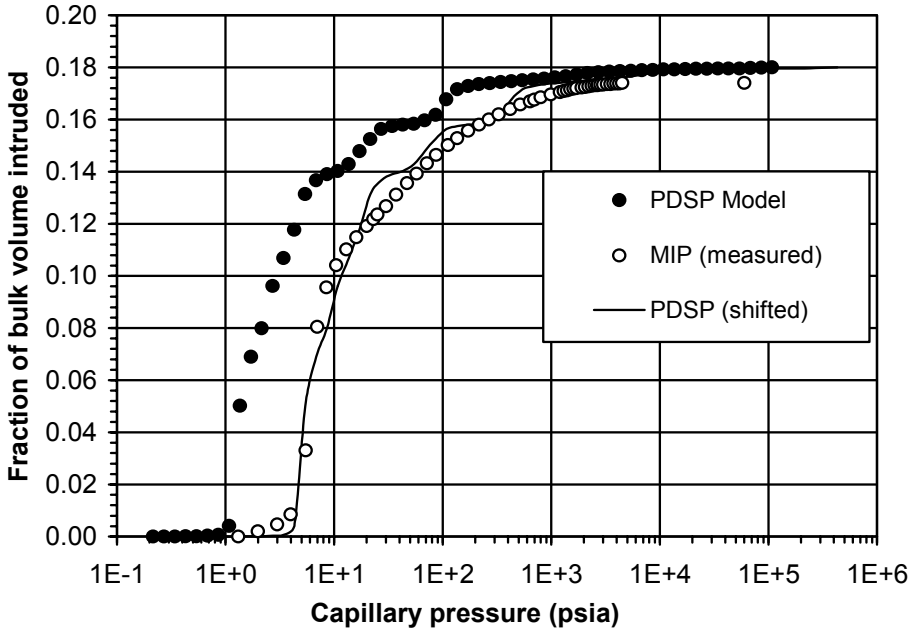

Figure 5. Estimation of mercury intrusion porosimetry curve from the PDSP pore size distribution.

result in the same value of total porosity, which is a remarkable result. In constructing the synthetic capillary pressure curve, pore accessibility effects (shielding of large pores by smaller ones) are ignored and entry capillary pressures are computed assuming cylindrical pore geometry. The two curves can be made to overlap if the pore entry radius is taken to be smaller than the pore radius by a factor of about four. This shifts the capillary pressure curve to the right. The shift is reasonable if one considers the existence of local constrictions (pore throats) in the pore space.

The measured decay of transverse magnetization in the water-saturated sample, shown in Figure 6, was analyzed in terms of a multi-exponential NMR relaxation model:

$$M(t) = M_o \sum_i f_i \exp(-t/T_{2,i}) \tag{9}$$

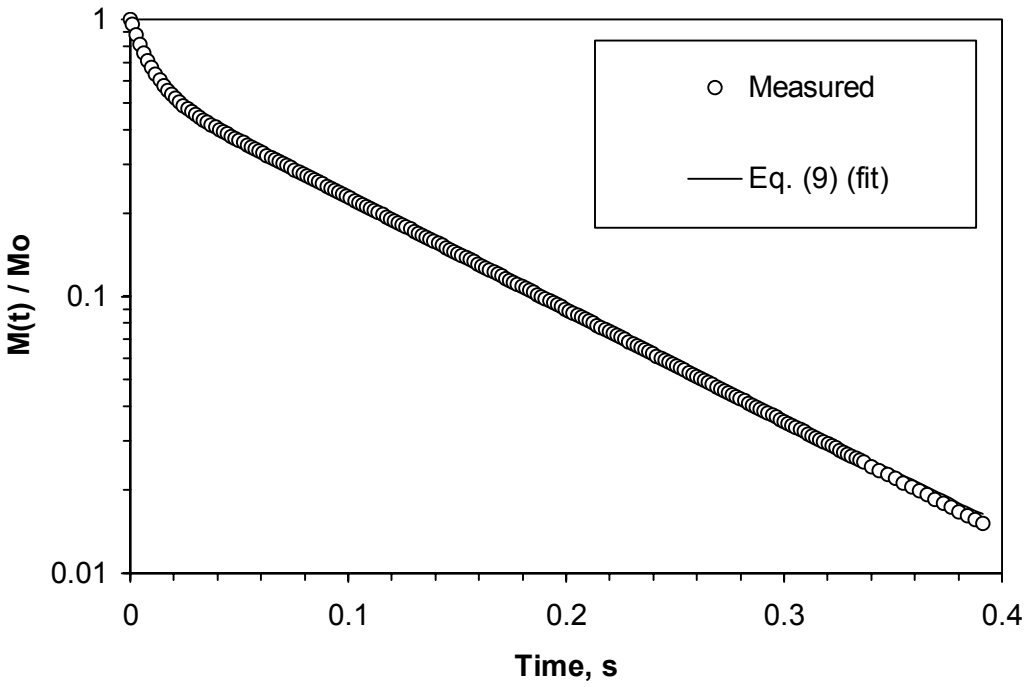

Figure 6. Transverse magnetization decay in water-saturated sample.

The results are shown in Figure 7 and demonstrate that magnetization decay is essentially bi-exponential. A fraction $f_{short} = 0.41$ of the protons in the water-saturated sample relax with characteristic time $T_{2,short} \approx 0.01\,s$, whereas the remaining fraction ($f_{long} = 0.59$) relaxes with characteristic time $T_{2,long} \approx 0.1\,s$. To interpret these results we adopt the following analysis of NMR relaxation in fractal pores (Sapoval *et al.*, 1996).

At distance L_{cg} from the walls, the Minkowski frontier delimits inner pore volumes of size L_{int}. Spins within a distance L_{cg} from the pore walls ('coarse-graining' length) diffuse easily to the surface and are relaxed with characteristic time $T_{2,short} \approx \frac{L_{cg}^2}{D_o}$, where $L_{cg} = \ell\left(\frac{\Lambda}{\ell}\right)^{1/(D-1)}$, $\Lambda = D_o/\rho$, D_o is the self-diffusion coefficient of water and ρ is the surface relaxivity. The fraction of magnetization that follows this rapid decay is $f_{short} = \left(\frac{L_{cg}}{\xi}\right)^{2-D}$, where ξ is the upper cutoff of the fractal region. Relaxation of spins within the inner pore volume is diffusion-controlled and has characteristic time $T_{2,long} \approx L_{int}^2 / (2\pi^2 D_o)$.

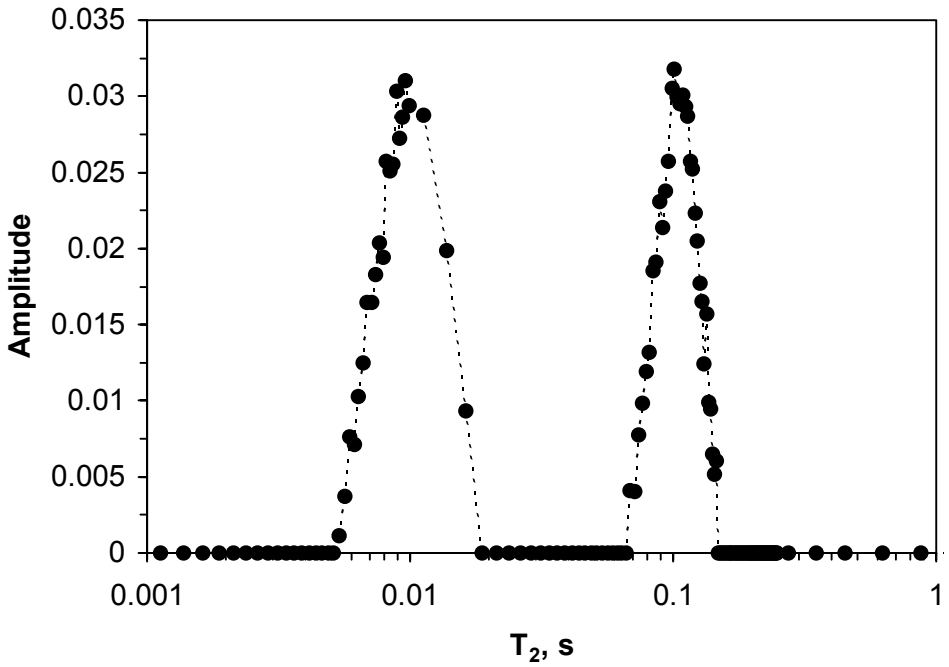

Figure 7. Distribution of transverse relaxation times for water saturated sample.

Using D = 2.47 and ℓ = 2 nm from SANS, $D_o = 2.5\times10^{-9}$ m^2/s, ρ = 12 μm/s (Slijkerman and Hofman, 1998) and for the experimentally observed relaxation times and peak intensities, the analysis of Sapoval *et al.* (1996) predicts $\xi = 35\,\mu m$ and $L_{int} \approx$ 72 μm. Hence, this theory explains the experimental NMR data in a manner entirely consistent

with our analysis of scattering data. Since for the above parameter values L_{cg} = 5.2 μm, we can independently estimate f_{short} from the SANS/USANS/BSEM-derived pore size distribution as:

$$f_{short} = \frac{\int_{R_{min}}^{L_{cg}} V(r)f(r)dr + \int_{L_{cg}}^{R_{max}} \left[V(r) - V(r - L_{cg})\right]f(r)dr}{\int_{R_{min}}^{R_{max}} V(r)f(r)dr} \qquad (10)$$

This calculation gives f_{short} = 0.48, in good agreement with the experimentally determined value. Finally, we estimate the length scale l_c (pore diameter) controlling permeability, using the following formula (Thompson *et al.*, 1987):

$$k = \frac{1}{226}\frac{l_c^2}{F} \qquad (11)$$

For k = 450 mD, $F = \phi^{-m}$ and $1.8 \le m \le 2$, we obtain l_c = 52 ± 4 μm, corresponding to a pore radius of 26 ± 2 μm. Our analysis shows that this length scale is within the fractal regime, very near the upper cutoff ξ. The mercury-air breakthrough capillary pressure, associated with the breakthrough radius, P_c^o = 4.2 ± 0.3 psia, in good agreement with the experimental data (see Figure 5).

CONCLUSIONS

We have presented the first complete multiscale statistical-geometric description of a natural porous sandstone, which is consistent with a host of experimental data and captures all length scales of relevance to capillary phenomena. The microstructure is fractal on length scales 2 nm to 40 μm and Euclidean on scales 40 μm to 500 μm. Remarkably, the majority of the pore volume (62%) is contributed by a surface fractal with dimension D = 2.47. The results from the neutron scattering, porosimetry and NMR experiments are quantitatively consistent with a model of very broad pore size distribution, as well as with a theoretical description of nuclear spin relaxation in a fractal medium. Our analysis gives new insights into the pore size distribution, porosity, correlation function and characteristic length scales for nuclear spin relaxation, permeability and capillary pressure. It also provides detailed input data for the computer simulation of the microstructure of reservoir rock.

REFERENCES

Broseta, D., Barre, L., Vizika, O., Shahidzadeh, N., Guilbaud, J.-P., and Lyonnard, S., "Capillary condensation in a fractal porous medium", Physical Review Letters, (2001) 86, no. 23, 5313-5316.

Bryant, S., Cade, C., and Mellor, D., "Permeability prediction from geologic models", American Association of Petroleum Geologists Bulletin, (1993) 77, no.8, 1338-1350.

Constantinides, G.N., and Payatakes, A.C., "Effects of precursor wetting films in immiscible displacement through porous media", Transport in Porous Media, (2000) 38, no. 3, 291-317.

Glinka, C.J., Rowe, J.M., and LaRock, J.G., "The small-angle neutron scattering spectrometer at the National Bureau of Standards", Journal of Applied Crystalography, (1986) 19, 427-439.

Hainbuchner, M., Villa, M., Kroupa, G., Bruckner, G., Baron, M., Amentisch, H., Seidl, E., and Rauch, H., "The new high-resolution ultra-small angle neutron scattering instrument at the High Flux Reactor in Grenoble", Journal of Applied Crystallography, (2000) 33, 851-854.

Ioannidis, M.A., Kwiecien, M.J, and Chatzis, I., "Statistical analysis of the porous microstructure as a method for estimating reservoir permeability", Journal of Petroleum Science and Engineering, (1996) 16, 251-261.

Kenyon, W.E., "Petrophysical principles of applications of NMR logging", The Log Analyst, (1997) 38, no. 2, 21-43.

Mildner, D.F.R., and Hall, P.L., "Small-angle scattering from porous solids with fractal geometry", Journal of Physics D: Applied Physics, (1986) 19, 1535-1545.

Radlinski, A.P., Radlinska, E.Z., Agamalian, M., Wignall, G.D., Lindner, P., and Randl, O.G., "Fractal Geometry of Rocks", Physical Review Letters, (1999) 82, 3078-3081.

Radlinski, A.P., Mastalerz, M., Hinde, A.L., Hainbuchner, M., Rauch, H., Baron, M., Lin, J.-S., Fan, L., and Thiyagarajan, P., "Non-invasive Measurements of Pore Size Distribution in Coal Pellets Using X-ray and Neutron Techniques", International Coalbed Methane Symposium 2001 Proceedings, May 14-18, University of Alabama Tuscaloosa, Alabama, USA, 163-175.

Sapoval, B., Russ, S., Petit, D., and Korb, J.P., "Fractal geometry impact on nuclear relaxation in irregular pores", Magnetic Resonance Imaging, (1996) 14, no. 7/8, 863-867.

Slijkerman, W.F.J., and Hofman, J.P., "Determination of surface relaxivity from NMR diffusion measurements", Magnetic Resonance Imaging, (1998) 16, no. 5/6, 541-544.

Song, Y.Q., Ryu, S.G., and Sen, P.N., "Determining multiple length scales in rocks", Nature, (2000) 406, no. 6792, 178-181.

Spanne, P., Thovert, J.-F., Jacquin, C., Lindquist, W., Jones, K., and Adler, P., "Synchrotron computed microtomography of porous media: topology and transports", Physical Review Letters, (1994) 73, 2001-2004.

Thompson, A.H., Katz, A.J., and Krohn, C.E., "The microgeometry and transport properties of sedimentary rock", Advances in Physics, (1987) 36, no.5, 625-694.